Fermi National Accelerator Laboratory

FERMILAB-Pub-93/153

A Simple Drift-Tube Telescope for Detector Tests

D.M. Kaplan, M. Apolinski and W. Luebke

Physics Department, Northern Illinois University
DeKalb, Illinois 60115

S.W.L. Kwan

Particle Detector Group, Fermi National Accelerator Laboratory
P.O. Box 500, Batavia, Illinois 60510

June 1993

Submitted to *Nuclear Instruments and Methods*

Operated by Universities Research Association Inc. under Contract No. DE-AC02-76CHO3000 with the United States Department of Energy

Disclaimer

A Simple Drift-Tube Telescope for Detector Tests

D. M. Kaplan, M. Apolinski,[a] and W. Luebke
Physics Dept., Northern Illinois University, DeKalb, IL 60115, USA

S. W. L. Kwan
Particle Detector Group, Fermi National Accelerator Laboratory, Batavia, IL 60510, USA

We have constructed and operated a telescope consisting of eight drift tubes with 60° stereo covering an aperture of 6.5 cm^2. The telescope provides position resolution of $\approx$ 100 μm RMS and angular resolution of $\approx$ 1/3 mrad. The small amount of electronics required and the relative simplicity of calibration make this an attractive approach for instrumenting detector tests when good positional and angular resolution are needed.

1. Introduction

In the course of detector development and testing, the need often arises for a simple means of tracking charged particles. Typically the device to be tested[1] is to be placed in a beam of charged particles in order to establish its efficiency and other performance measures such as position or time resolution. The paths of charged particles traversing a given fiducial volume and passing through the device are to be reconstructed to some desired accuracy.

We have devised a design for single-wire drift tubes which lends itself to such applications. A telescope of eight such tubes (see Figures 1 and 2) has been constructed and used for a detector test in the copious muon flux behind Experiment 789 in Fermilab's Meson East laboratory. The tubes are grouped in two sets of four surrounding a 16.6-cm gap in which the device under test is placed. To provide comparable resolutions in x and in y, the tubes are oriented in three views at 60° stereo. The fourth tube in each set provides additional redundancy in a view, such that one view is measured by two tubes while the other two are measured by three tubes each. A trigger is provided by two 2.5 $\times$ 2.5-cm^2 scintillation counters located at either end of the telescope; to ensure that the muons detected are of sufficient energy to undergo little scattering in the detectors, a third counter 30 $\times$ 30 cm^2 in size, located behind 4.6 m of shielding concrete, is placed in coincidence with the first two.

2. Drift tube design and construction

Each tube (see Figure 3) is constructed from a length of rectangular extruded 6061 T6 aluminum 5.1 $\times$ 7.6 cm^2 in cross section with walls 0.32 cm thick. Cut to a length of 15 cm, the tube is closed off with aluminum end plates, through which holes 2.5 cm in diameter have been bored to receive plastic plugs. The anode wire, consisting of nickel-struck gold-plated tungsten of 50-μm diameter and tensioned to 200 g, is soldered and glued to a gold-plated brass pin inserted into each plug [2]. An additional through-hole in each end plate, drilled

[1] in this instance a MgF_2 crystal used to study total internal reflection of Cherenkov light; see ref. [1].

and tapped for an 1/8"-thread barbed pipe nipple, provides for gas connections, and two blind holes drilled and tapped for 4-40 machine screws are used to mount the electrical service box (described below). The plug hole, and hence the anode wire, is offset by 1.0 cm relative to the center of the end plate, for two reasons: 1) to ensure that the wires in the three stereo views enclose a triangle rather than crossing at a point in order to break the drift-direction ambiguity, and 2) to leave sufficient room for the gas connections. The inner edges of the end plates are relieved to a depth of 1.6 mm to fit snugly inside the tube. To reduce scattering of traversing particles, a hole of 5.5-cm diameter is bored in the two side faces of the tube, to be covered over with aluminized mylar; to avoid sharp corners which might concentrate the electric field and cause breakdown, the inner edge of this hole is given a 3-mm radius. Flanking this hole are two blind alignment holes of 3.2-mm diameter, located on a line oriented at 30° with respect to the long axis of the tube; adjacent tubes are mounted to each other by means of dowel pins press-fit into these alignment holes, thereby ensuring the 60° stereo angle.

Prior to assembly, all aluminum parts are cleaned thoroughly with ethyl alcohol. The end plates are then glued to the tube using Scotch-Weld 2216 epoxy. After the epoxy has cured, the anode wire is inserted, soldered at one end, tensioned, soldered at the other end, and glued with Epon 828 epoxy. Finally, the aluminized mylar windows are stretched flat and epoxied to the side faces. A thin bead of Tra-Duct 2902 conductive epoxy surrounding the hole grounds the window electrically, and an additional bead of Epon 828 reinforces the joint.

Electrical connections to the tube are provided by a service box mounted to one end plate (Figure 4). We use a Bud two-piece "Minibox" chassis made of bent sheet aluminum (Bud CU-2100B). A hole of 3.2-cm diameter is bored in one end of the box to fit over the end of the plastic plug, flanked by two 4-40 clearance holes for the mounting screws. The opposite end of the box is fitted with a high-voltage coaxial bulkhead jack (Kings 1704-1), electrically insulated from the box by means of a rectangular piece of 1.6-mm FR-4 sheet. A 1 MΩ 2-watt carbon-composition resistor is soldered to the jack at one end and to a socket (AMP M series) at the other, such that the socket slides onto the anode pin when the service box is mounted against the end plate. All solder joints are sheathed in plastic shrink tubing to reduce the chance of breakdown. To break the ground loop and reduce noise pick-up, the high-voltage ground is connected to the service box via a 100 Ω 1/4-watt resistor. The signal is brought out through a 1000 pF 7.5 kV ceramic capacitor to a coaxial connector (Kings 1074-1) mounted in the sidewall of the box. A prototype service box was tested up to 4 kV without breakdown. Positive high voltage is supplied to the anode wires via the service box from a 2-channel Kiebler 6900 power supply; each channel supplies four wires in parallel.

The tubes are connected in series by short lengths of Tygon tubing and operated in a mixture of 50% argon/50% ethane. A gas flow rate of 0.02 lpm is found to suffice for efficient operation of the tubes. An overpressure of $\approx$ 1 mm of H_2O is maintained by an oil-filled output bubbler.

A mounting stand holds the tubes in line to $\approx$ 1 mm, with each set of four tubes sandwiched between two 6-mm-thick aluminum plates supported on two 6-mm-diameter threaded rods. To minimize the amount of material in the aperture, holes of 5.5-cm diameter were bored in these plates to line up with the mylar windows of the tubes. (Since these plates support the glue joints of the outermost tubes' mylar windows against the gas overpressure,

it is desirable that the holes match the 5.5-cm windows rather than being oversized. Internal windows' glue joints are supported by the face of the adjacent tube.) Bowing of the threaded rods results in relative alignment errors of the tubes. Additional sources of error include variations in hole locations in the (hand-machined) parts. Alignment errors are calibrated out by careful analysis of the reconstructed tracks.

3. Electronics and readout system

From the service box, the signal is transported by a 3-ns RG174 cable to a Nanometric Systems N-277-C 16-channel amplifier/discriminator card. Short lengths of 0.6-cm copper braid ground the service boxes to each other and to the amplifier/discriminator card. The discriminators' differential-ECL output signals are sent via 60 m of "Twist-n-Flat" ribbon cable to a LeCroy 2229 8-channel TDC housed in a CAMAC crate. The CAMAC crate is interfaced to an IBM PC via a DSP 6002 crate controller. The TDC's conversion gain is set to 2 counts/ns, giving a full-scale range of 1023 ns; since within the fiducial region of the trigger counters, the maximum drift distance is < 4 cm, and the drift velocity is ≈ 50 μm/ns, this is adequate.

The data-acquisition trigger is formed using LeCroy NIM logic. Signals from the three scintillation counters are discriminated and placed in three-fold coincidence; to minimize time jitter, the cable lengths are selected such that the signals from the small counters arrive later than that from the large counter and thus determine the time of the coincidence. The coincidence triggers two gate generators in series; the first is set to provide 4.4 ms deadtime, so that a second trigger can not occur during the readout cycle. The TDC's conversion cycle is started by the output of the second gate generator, and each TDC channel is stopped by receipt of a discriminated pulse from a drift tube. The resulting LAM condition in the TDC causes the PC to carry out a readout cycle. The data acquisition program loops until LAM is detected, whereupon it reads out the eight drift times (plus whatever other data are required for the device under test) and stores them in memory. When a sufficient number of events have been accumulated, they are written to the hard disk.

4. Performance

Figure 5 shows efficiency vs. high voltage for a typical drift tube. The efficiency is seen to plateau at $\approx$ 2.85 kV. Operated at 2.9 kV the tubes were found to have a rather nonlinear relationship between drift time and distance; this was much alleviated at 3.1 kV, which was therefore the voltage selected for most of the data-taking. At this voltage very little quiescent current was drawn by the tubes ($\approx$40 nA per tube). Figure 6 shows the time-distance relationship obtained from the data at 3.1 kV. For all of these data the discriminator threshold was set to 1.37 V, corresponding to a threshold signal current of $\approx$ 1.37 μA on the anode wire.

Since the efficiencies are so close to 100%, trackfitting is performed only for events in which all eight TDC channels report non-overflow values. For each such "8-hit" event, the eight drift-direction ambiguities lead to 256 possible interpretations. For each interpretation, a three-dimensional least-squares fit is performed with four parameters: the positions in x and y at $z = 0$ (the center of the telescope) and the slopes dx/dz and dy/dz. (The z axis

is along the approximate direction of particle travel and forms a right-handed coordinate system with x and y.) Of the 256 possible interpretations, the one interpretation which minimizes χ^2 is chosen. If the χ^2 probability is less than 0.01 the event is ignored. Figure 7 shows the distribution of the residual of a typical tube, defined as the difference, in the coordinate measured by the tube, of the fitted position from the measured position. It is seen to be $< 100\,\mu$m wide RMS, indicating the good position resolution achieved. (Due to the small number of points in the track fit, the actual measurement error is $\approx 17\%$ larger than this.) Figure 8 shows the RMS residual vs. distance of the fitted track from the wire.

Acknowledgements

We thank C. N. Brown, H. Jöstlein, and K. M. Kephart of Fermilab for useful discussions, and P. Stone of Northern Illinois University for his contributions to the mechanical design and his machining of the parts. We also thank the members of Fermilab's Particle Detector Group, who provided many of the components of the data acquisition system. This work was supported in part by a grant from the U. S. Department of Energy.

References

[a] Present address: Physics Department, Louisiana State University, Baton Rouge, LA 70803, USA.

[1] D. M. Kaplan *et al.*, Nucl. Instr. & Meth. A330 (1993) 33.

[2] The plugs and pins are of the type developed for the D0 Muon Detector proportional drift tubes; see C. Brown *et al.*, Nucl. Instr. and Meth. A279 (1989) 331.

Figure captions

FIGURE 1. Layout of drift-tube telescope; the shielding concrete and downstream trigger scintillation counter are not shown.

FIGURE 2. Photograph of drift-tube telescope.

FIGURE 3. Details of drift-tube components (all dimensions in mm): a) tube body, b) end plate.

FIGURE 4. Details of service box (all dimensions in mm).

FIGURE 5. Efficiency vs. high voltage for a typical tube.

FIGURE 6. Time-distance relation for a typical tube (at 3.1 kV); note the nonlinearity. The curve superimposed on the data points represents the best-fit function $d = 0.5928 + 0.0445t - 1.926 \times 10^{-5}t^2$, where d is in mm and t in ns.

FIGURE 7. Residual distribution (as described in text) for a typical tube.

FIGURE 8. RMS residual vs. drift distance.

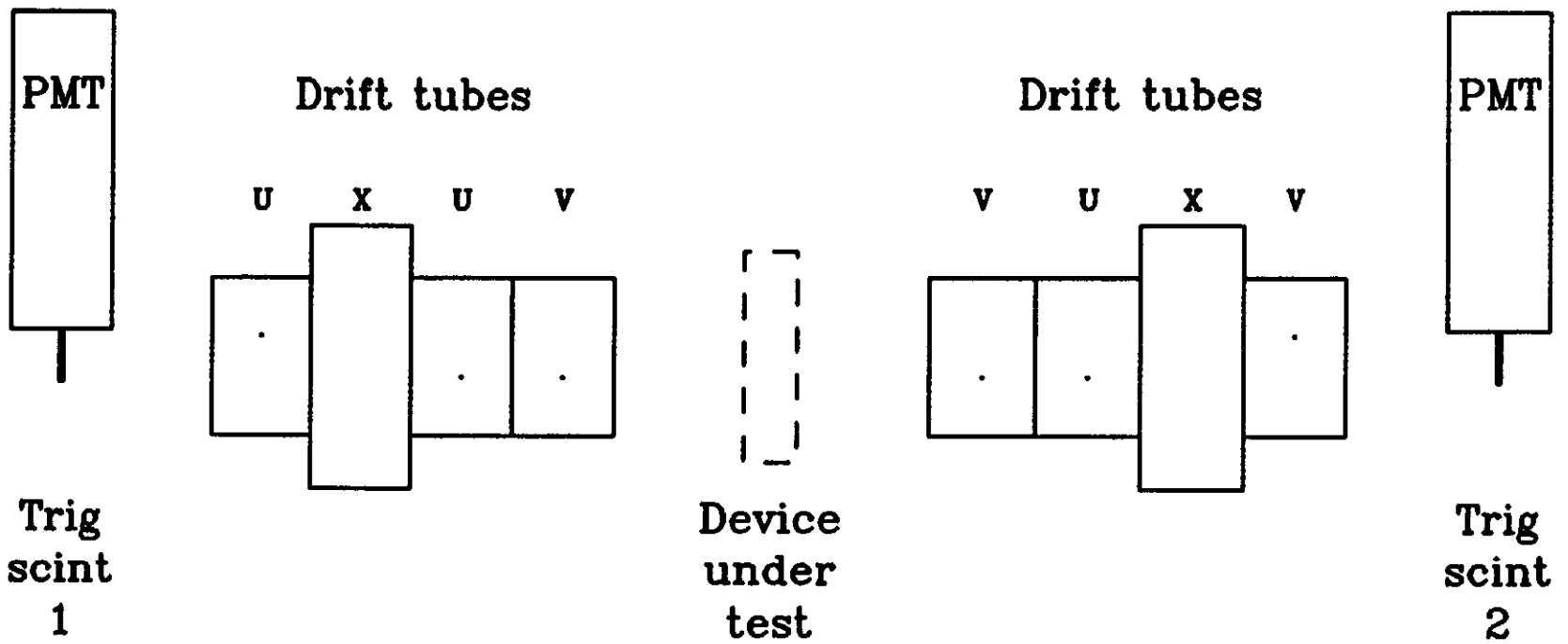
PMT
Drift tubes
U X U V
Drift tubes
V U X V
PMT
Trig scint 1
Device under test
Trig scint 2

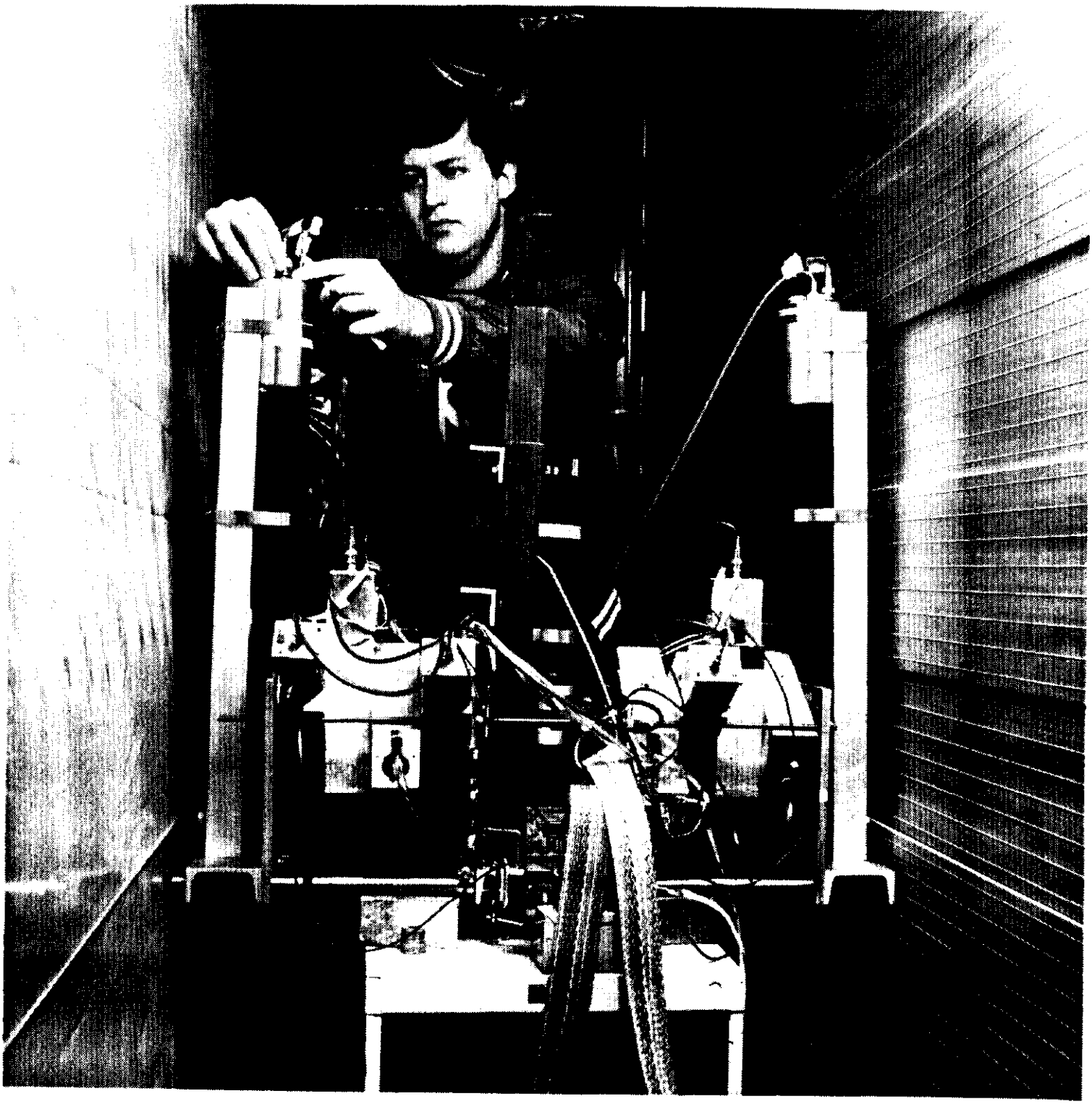

Drift Chamber Main Body

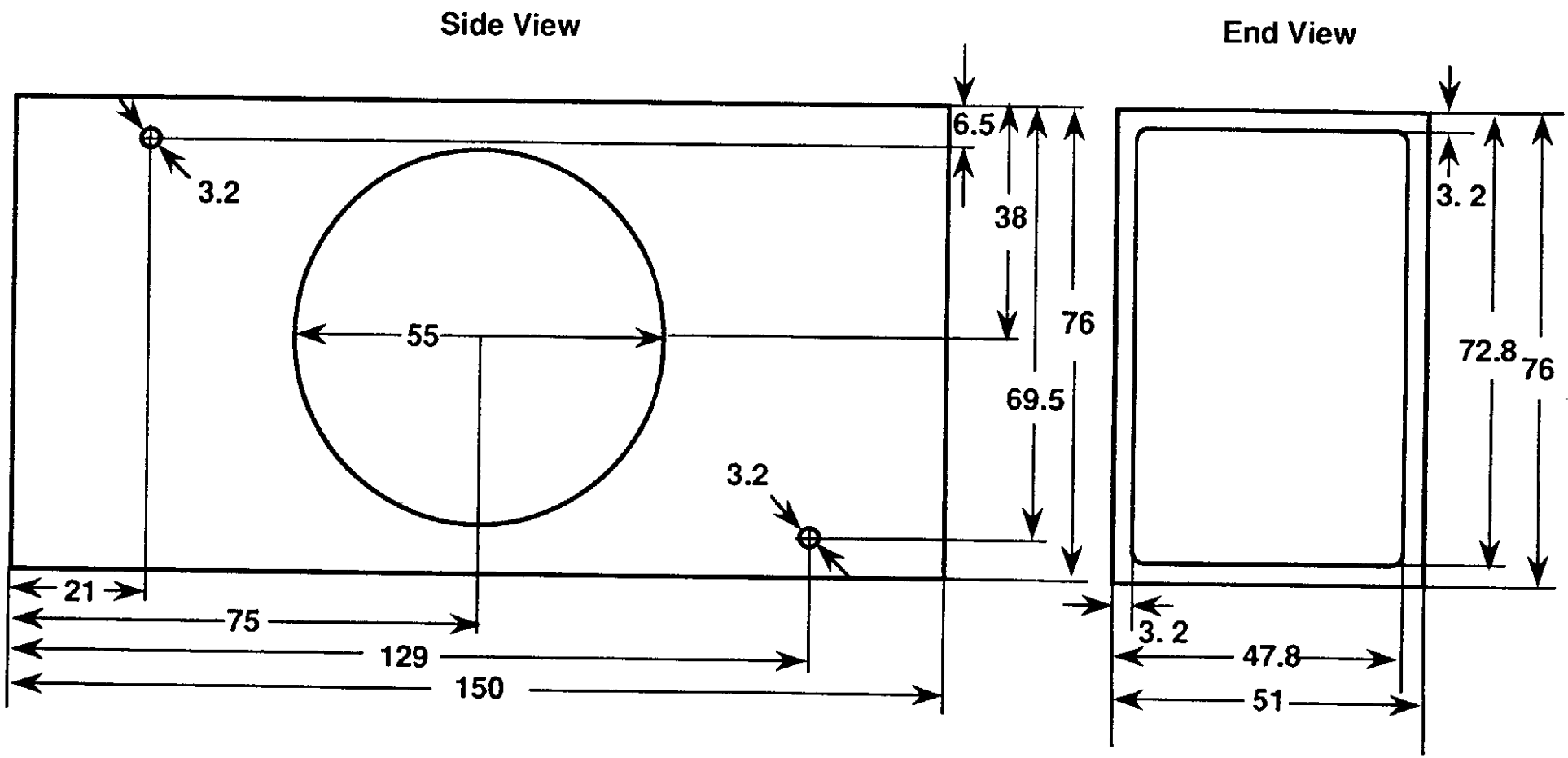

End Plate

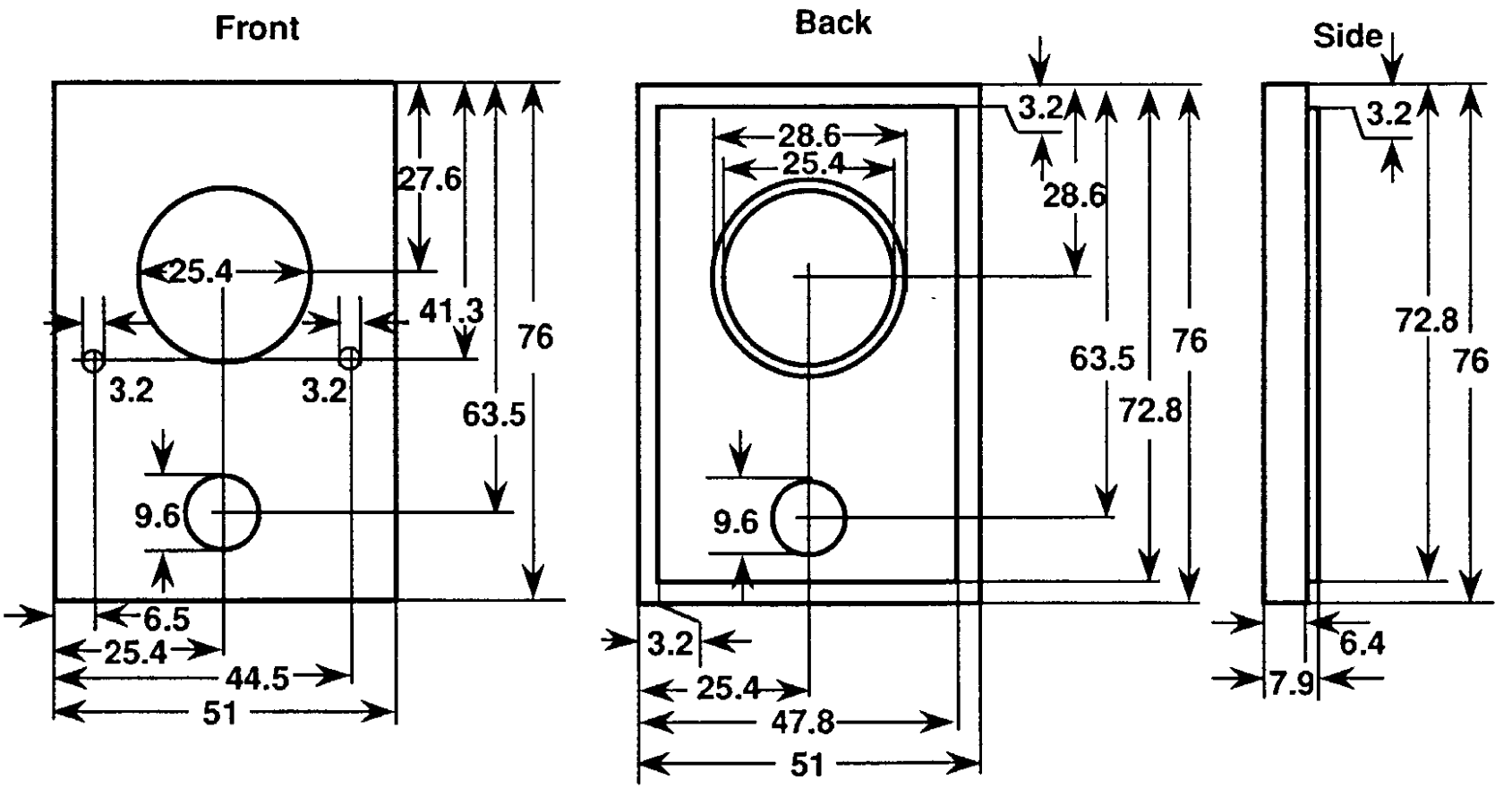
Front
Back
Side
27.6
25.4
41.3
76
3.2
3.2
63.5
9.6
6.5
25.4
44.5
51
28.6
25.4
3.2
28.6
63.5
76
72.8
9.6
3.2
25.4
47.8
51
3.2
72.8
76
6.4
7.9

Service box

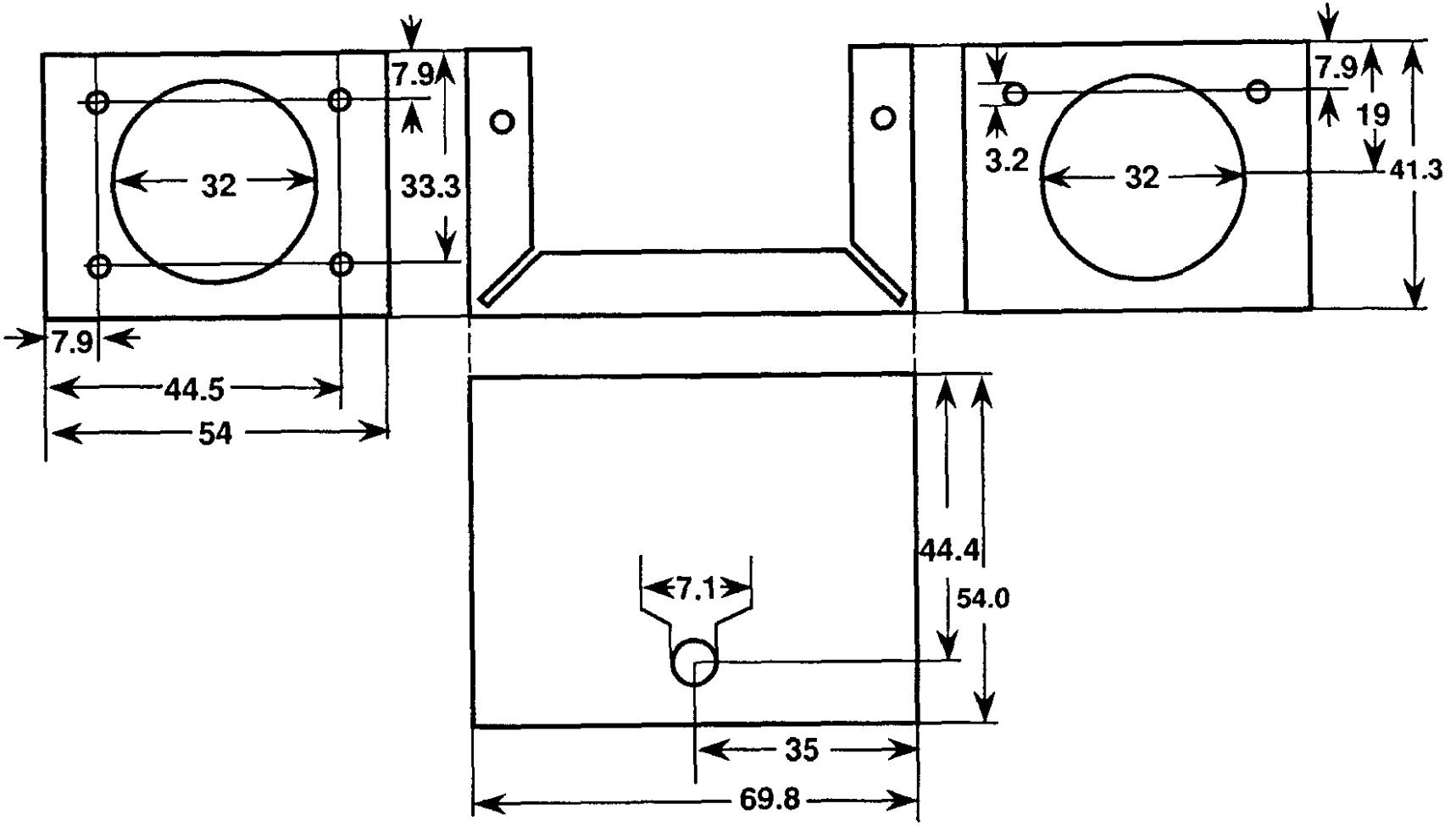

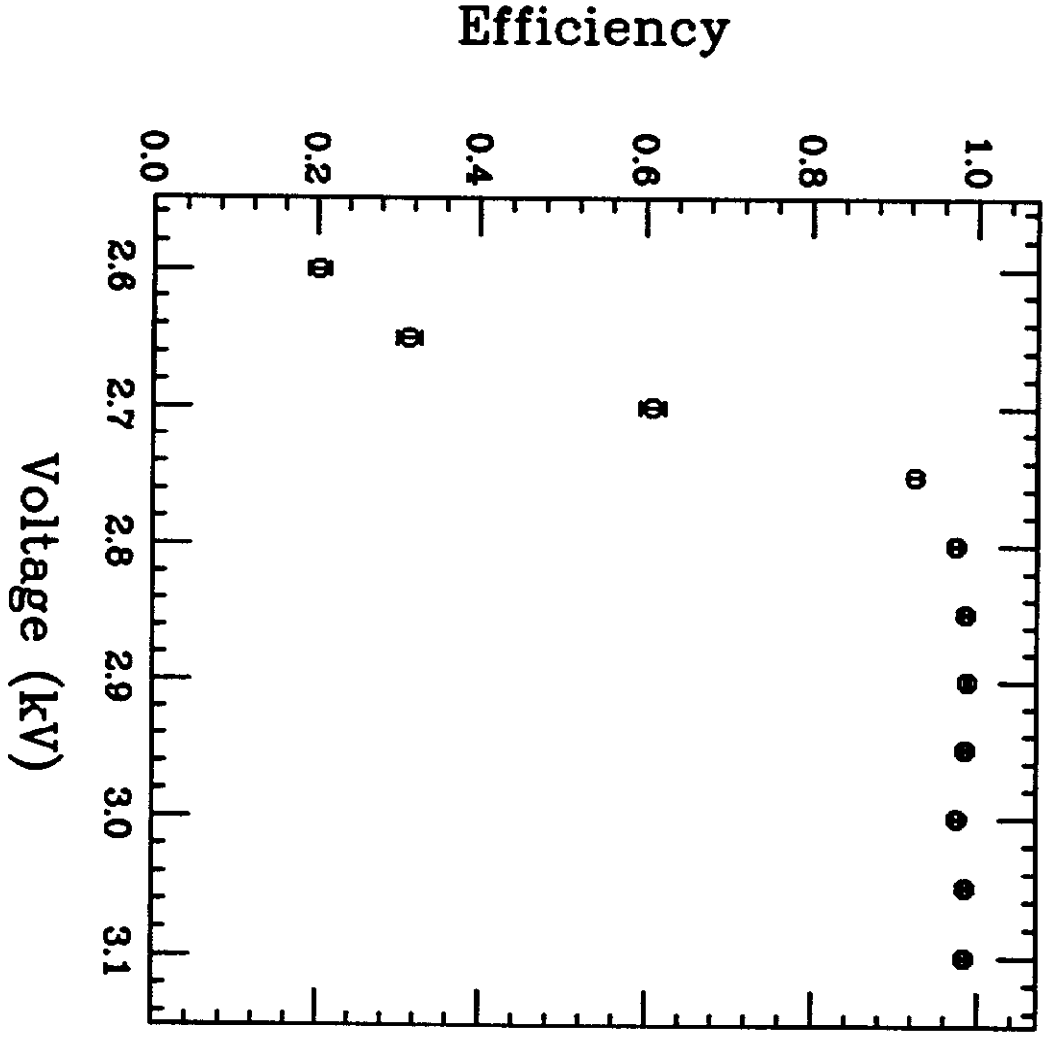
Efficiency
0.0
0.2
0.4
0.6
0.8
1.0
2.6
2.7
2.8
2.9
3.0
3.1
Voltage (kV)

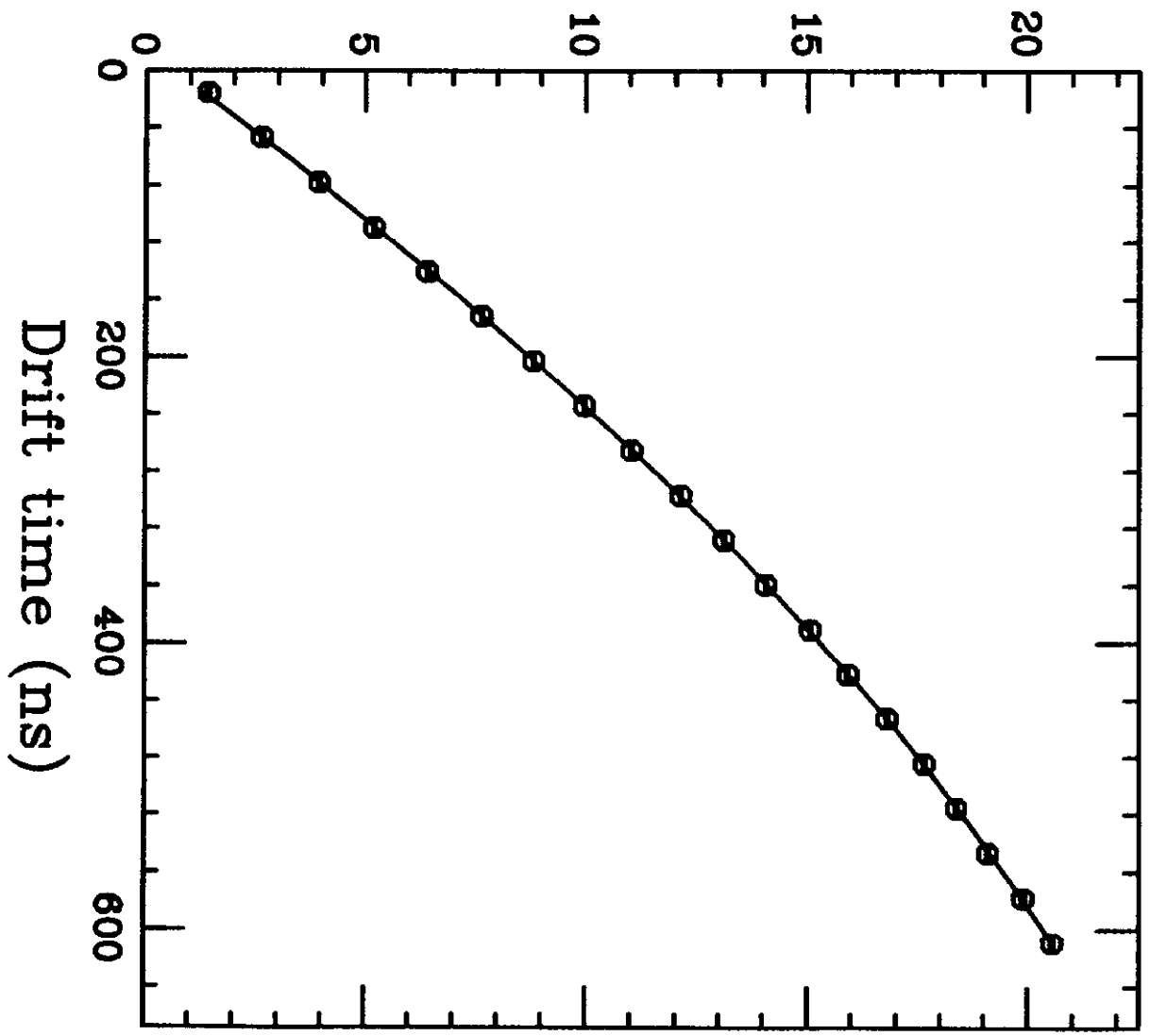
Drift distance (mm)
Drift time (ns)
0
5
10
15
20
0
200
400
600

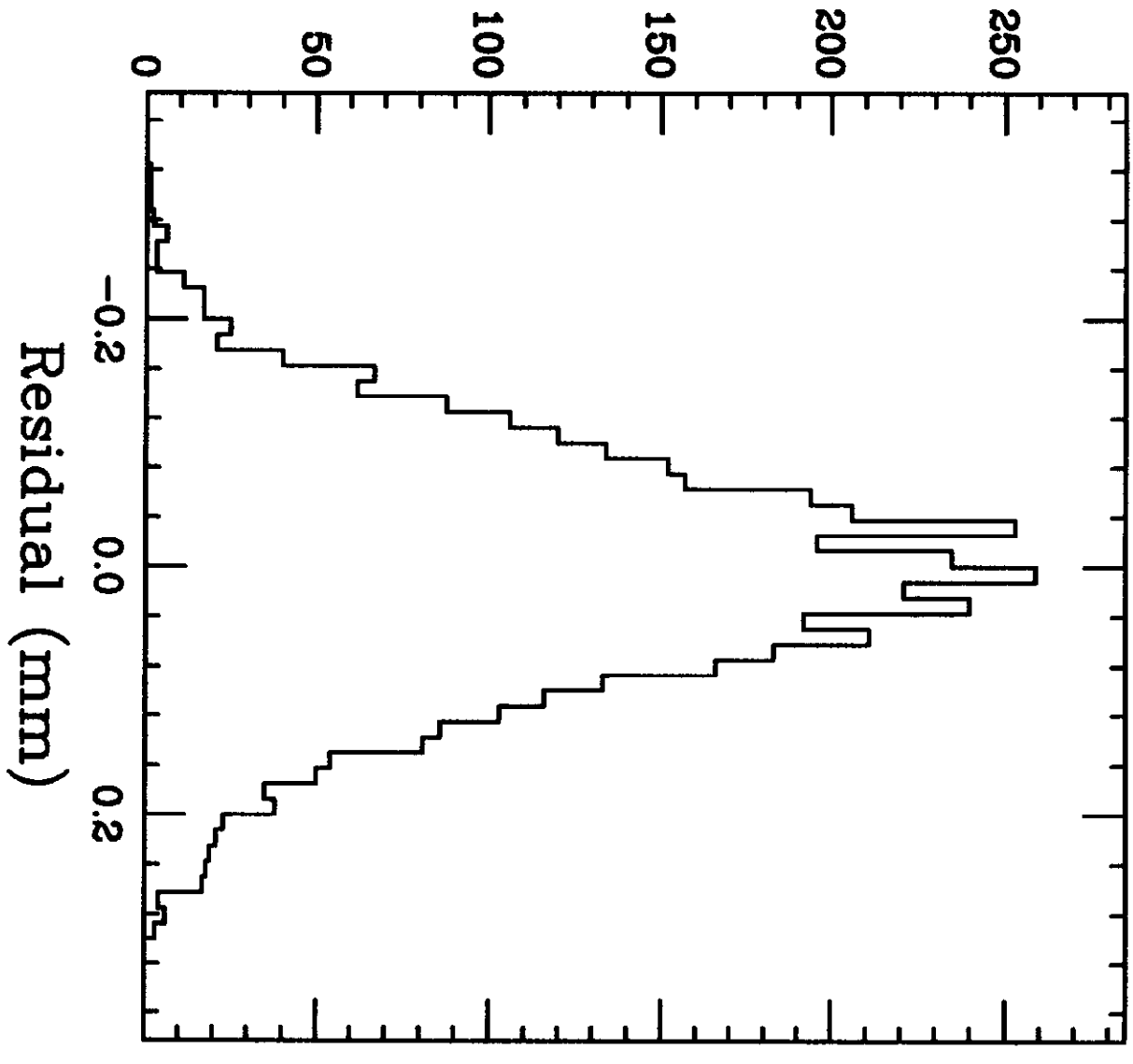
Events
0
50
100
150
200
250
Residual (mm)
-0.2
0.0
0.2

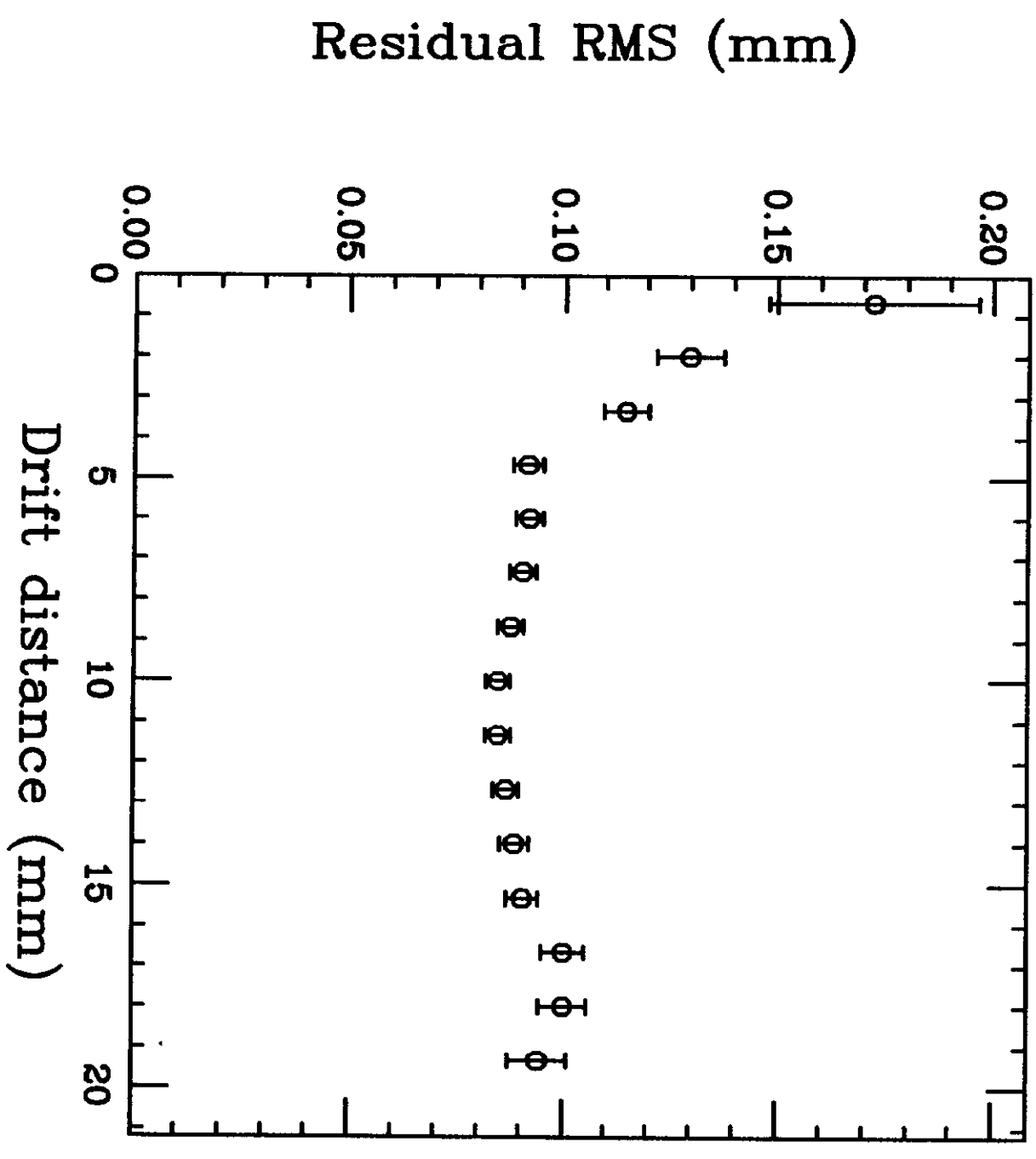
Residual RMS (mm)
0.00
0.05
0.10
0.15
0.20
0
5
10
15
20
Drift distance (mm)